Smart Materials and Devices

https://doi.org/10.70401/smd.2025.0001

Supplementary information

Terphenyl-modified diboron embedded multi-resonance thermally activated delayed fluorescence emitters with high efficiency

Fu-Ming Liu, Zhi-Hao Qu, Peng Zuo, Yue-Jian Yang, Jian-Rong Wu, Liang-Sheng Liao, Dong-Ying Zhou, Zuo-Quan Jiang

Synthesis routes and details

Intermediate 2[1,2], 4[3], was synthesized according to the literature procedures. All other reagents and solvents are used from commercial sources without further purification.

Synthesis of 5-bromo-*N*,*N*,6'-triphenyl-[1,1':2',1"-terphenyl]-3-amine (3).

Compound 3,5-dibromo-N,N-diphenylaniline (10.00 g, 24.81 mmol), 2-([1,1':3',1"-terphenyl]-2'-yl)-4,4,5,5-tetramethyl-1,3,2-dioxaborolane (2) (10.61g, 29.77 mmol), tetrakis(triphenylphosphine)palladium (2.87g, 2.48 mmol) and potassium hydroxide (6.96g, 124.03 mmol) were dissolved in tetrahydrofuran (100 mL) and H_2O (20 mL) under a nitrogen atmosphere. After stirring at 80 °C for 15 h, the reaction was filtered, the solvent removed under vacuum condition, and then the residue purified by column chromatography on silica gel using petroleum ether/dichloromethane (3/1, v/v) as eluent, white solid was finally obtained. Yield: 7.65 g (55.81%). ^{1}H NMR (400 MHz, DMSO-d_6) δ 7.57-7.46 (m, 1H), 7.42-7.27 (m, 8H), 7.23 (dd, *J* = 8.4, 7.3 Hz, 4H), 7.12 -7.00 (m, 6H), 6.64 (dd, *J* = 7.1, 5.8 Hz, 6H), 6.50 (s, 1H). ^{13}C NMR (101 MHz, Chloroform-*d*) δ 147.87, 146.96, 142.53, 141.65, 141.36, 137.64, 129.89, 129.38, 129.31, 128.34, 127.81, 127.73, 126.50, 125.22, 124.20, 124.10, 123.04, 121.70. MS (EI) m/z: 552.41 [M+]. Calcd for $C_{36}H_{26}BrN$: 552.52.

Synthesis of N^3,N^3"-(1,3-phenylene)bis(N^3-(2,6-difluorophenyl)-N^5,N^5,6'-triphenyl-[1,1':2',1"-terphenyl]-3,5-diamine) (6).

Compound 3 (7.32 g, 13.24 mmol), N^1,N^3-bis(2,6-difluorophenyl)benzene-1,3-diamine (4) (2.00 g, 6.02 mmol), tris(dibenzylideneacetone)palladium(0) (551.15 mg, 601.86 μmol), dicyclohexyl(2',4',6'-triisopropyl-[1,1'-biphenyl]-2-yl)phosphane (573.85 mg, 1.2 mmol) and sodium tert-butoxide (3.47 g, 36.11 mmol) were dissolved in toluene (200 mL) under a nitrogen atmosphere. After stirring at 120 °C for 5 h, the reaction was filtered, the solvent removed under vacuum condition, and then the residue purified by column chromatography on silica gel using petroleum ether/dichloromethane (2/1, v/v) as eluent, white solid was finally obtained. Yield: 4.61 g (60.05%). ^{1}H NMR (400 MHz, Chloroform-*d*) δ 7.45-7.36 (m, 6H), 7.30-7.29 (m, 6H), 7.19-7.07 (m, 18H), 6.93 -6.81 (m, 13H), 6.75 (s, 4H), 6.73 (s, 3H), 6.43 (d, *J* = 10.4 Hz, 4H), 6.36 (s, 2H), 6.28 (d, *J* = 7.1 Hz, 2H), 6.11 (s, 2H), 6.05 (d, *J* = 8.1 Hz, 2H). ^{13}C NMR (101 MHz, Methylene Chloride-d_2) δ 162.64, 162.59, 160.13, 160.08, 159.22, 159.16, 156.76, 156.71, 148.92, 148.61, 148.01, 147.31, 145.51, 143.14, 142.90, 142.79, 140.18, 131.24, 130.70, 130.32, 130.23, 128.93, 128.71, 128.26, 128.16, 128.06, 127.57, 124.78, 124.63, 124.54, 123.74, 123.59, 123.54, 121.64, 120.46, 120.31, 117.74, 113.81, 113.76, 113.58, 113.32, 113.21, 113.15, 113.04, 112.98, 110.06, 108.43.MS (EI) m/z: 1275.81 [M+]. Calcd for $C_{90}H_{62}F_4N_4$:1275.51.

Synthesis of N^3,$N^{3''}$-(1,3-phenylene)bis(N^3,N^5,N^5,6'-tetraphenyl-[1,1':2',1''-terphenyl]-3,5-diamine) (7)

Using a similar synthetic procedure for compound 6, white solid was finally obtained. Yield: 3.6 g (59.08%). ^{1}H NMR (400 MHz, Methylene Chloride-d_2) δ 7.47–7.27 (m, 20H), 7.16–7.12 (m, 12H), 7.10 (s, 2H), 7.07–7.02 (m, 4H), 6.95–6.88 (m, 5H), 6.85–6.81 (m, 2H), 6.72 (d, *J* = 7.9 Hz, 8H), 6.62–6.53 (m, 5H), 6.42–6.30 (m, 6H), 6.22 (d, *J* = 8.1 Hz, 2H). ^{13}C NMR (101 MHz, Methylene Chloride-d_2) δ 147.82, 147.65, 147.37, 147.26, 147.12, 142.06, 141.63, 141.42, 138.99, 129.99, 129.64, 128.94, 128.89, 128.80, 127.61, 127.35, 126.28, 123.44, 122.88, 122.65, 122.57, 122.21, 121.76, 119.37, 119.03, 118.30, 29.69. MS (EI) m/z: 1203.67 [M+]. Calcd for $C_{90}H_{66}N_4$: 1203.55.

Synthesis of DTPF-ν-DABNA.

Boron tribromide (8.16 mL, 84.67 mmol) was added to a solution of Compound 6 (4.5 g, 3.53 mmol) in *o*-dichlorobenzene (60 mL) at room temperature under a nitrogen atmosphere. After stirring at 200 °C for 20 h, the reaction mixture was allowed to cool to room temperature. After addition of *N*,*N*-diisopropylethylamine (55.31 mL, 317.52 mmol) at 0 °C, the solvent was removed in vacuo, and then the residue purified by column chromatography on silica gel using petroleum ether/dichloromethane (2/1, v/v) as eluent, orange solid was finally obtained. Yield: 2.73 g (59.94%). ^{1}H NMR (400 MHz, Methylene Chloride-d_2) δ 10.43 (s, 1H), 9.16 (d, *J* = 7.8 Hz, 2H), 7.57 (d, *J* = 7.7 Hz, 6H), 7.46 (t, *J* = 7.0 Hz, 2H), 7.43–7.32 (m, 6H), 7.30 (d, *J* = 7.2 Hz, 4H), 7.22–7.07 (m, 12H), 6.98 –6.83 (m, 16H), 6.71 (d, *J* = 7.6 Hz, 2H), 5.86–5.76 (m, 4H), 5.64 (s, 1H). ^{13}C NMR (101 MHz, Methylene Chloride-d_2) δ 160.94, 158.45, 158.41, 149.30, 147.64, 145.85, 144.38, 143.71, 141.84, 141.68, 141.63, 139.36, 134.97, 131.01, 130.94, 130.27, 129.52, 129.33, 128.14, 127.69, 127.33, 126.21, 120.03, 117.18, 112.90, 112.68, 111.83, 108.03, 98.72. MS (EI) m/z: 1291.35 [M+]. Calcd for $C_{90}H_{56}B_2F_4N_4$: 1291.08.

Synthesis of DTP-ν-DABNA.

Using a similar synthetic procedure for DTPF-ν-DABNA, orange solid was finally obtained. Yield: 1.8 g (51.26%). ^{1}H NMR (400 MHz, Methylene Chloride-d_2) δ 10.42 (s, 1H), 9.17 (d, *J* = 6.0 Hz, 2H), 7.62–7.53 (m, 6H), 7.47–7.42 (m, 2H), 7.40–7.27 (m, 14H), 7.18 (d, *J* = 7.3 Hz, 12H), 6.94–6.85 (m, 12H), 6.69 (d, *J* = 8.6 Hz, 2H), 6.61 (d, *J* = 6.3 Hz, 4H), 5.73 (d, *J* = 17.8 Hz, 4H), 5.55 (s, 1H). ^{13}C NMR (101 MHz, Methylene Chloride-d2) δ 150.00, 147.68, 145.87, 145.75, 143.58, 143.01, 141.90, 141.79, 141.67, 141.28, 139.68, 134.97, 130.94, 130.76, 130.54, 130.32, 129.71, 129.55, 129.48, 128.04, 127.67, 127.57, 127.25, 126.03, 124.14, 119.86, 117.05, 114.96, 110.38, 110.01, 103.05. MS (EI) m/z: 1219.28 [M+]. Calcd for $C_{90}H_{60}B_2N_4$: 1219.12.

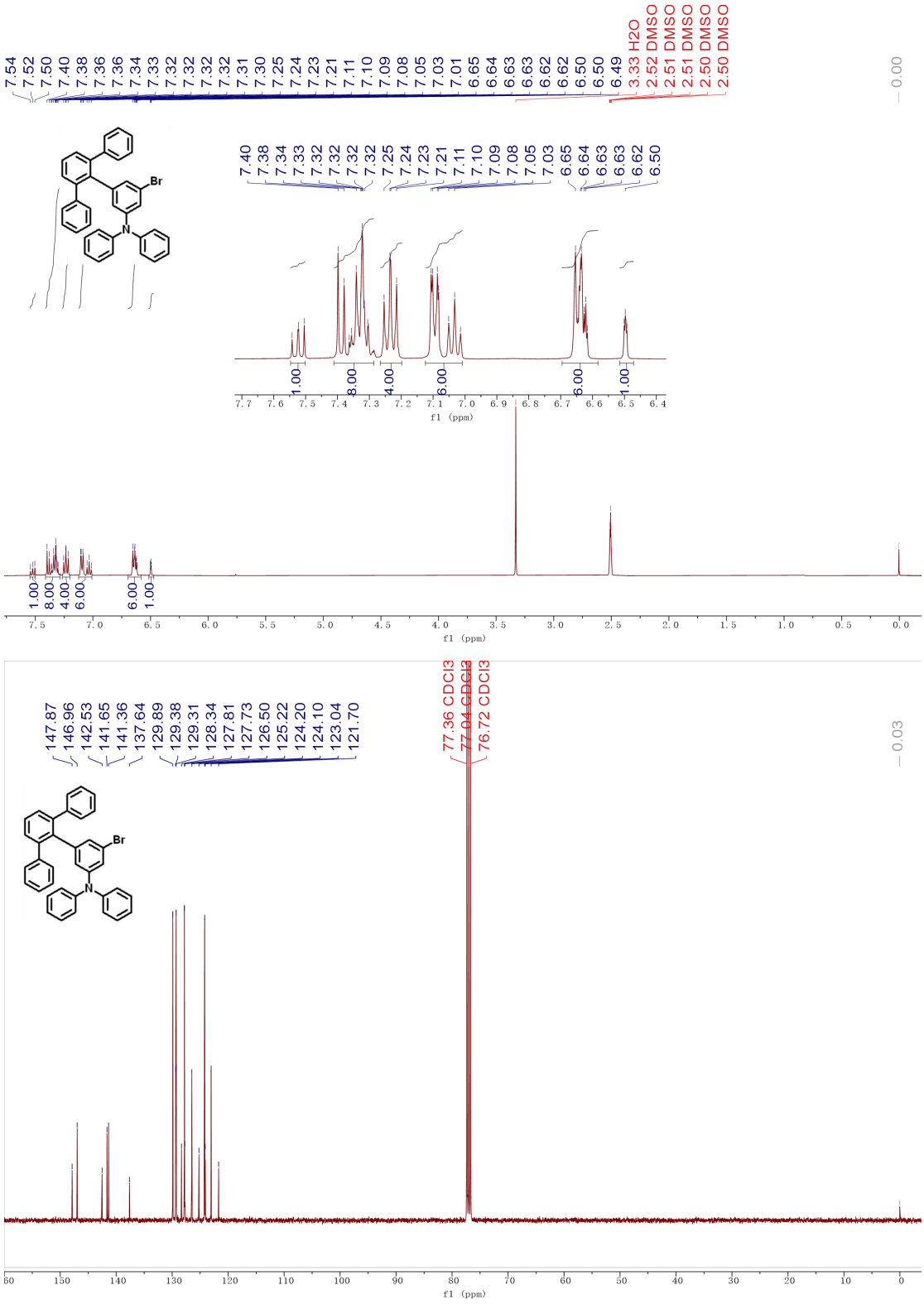

Figure S1. ^{1}H NMR and ^{13}C NMR spectrum of compound 4.

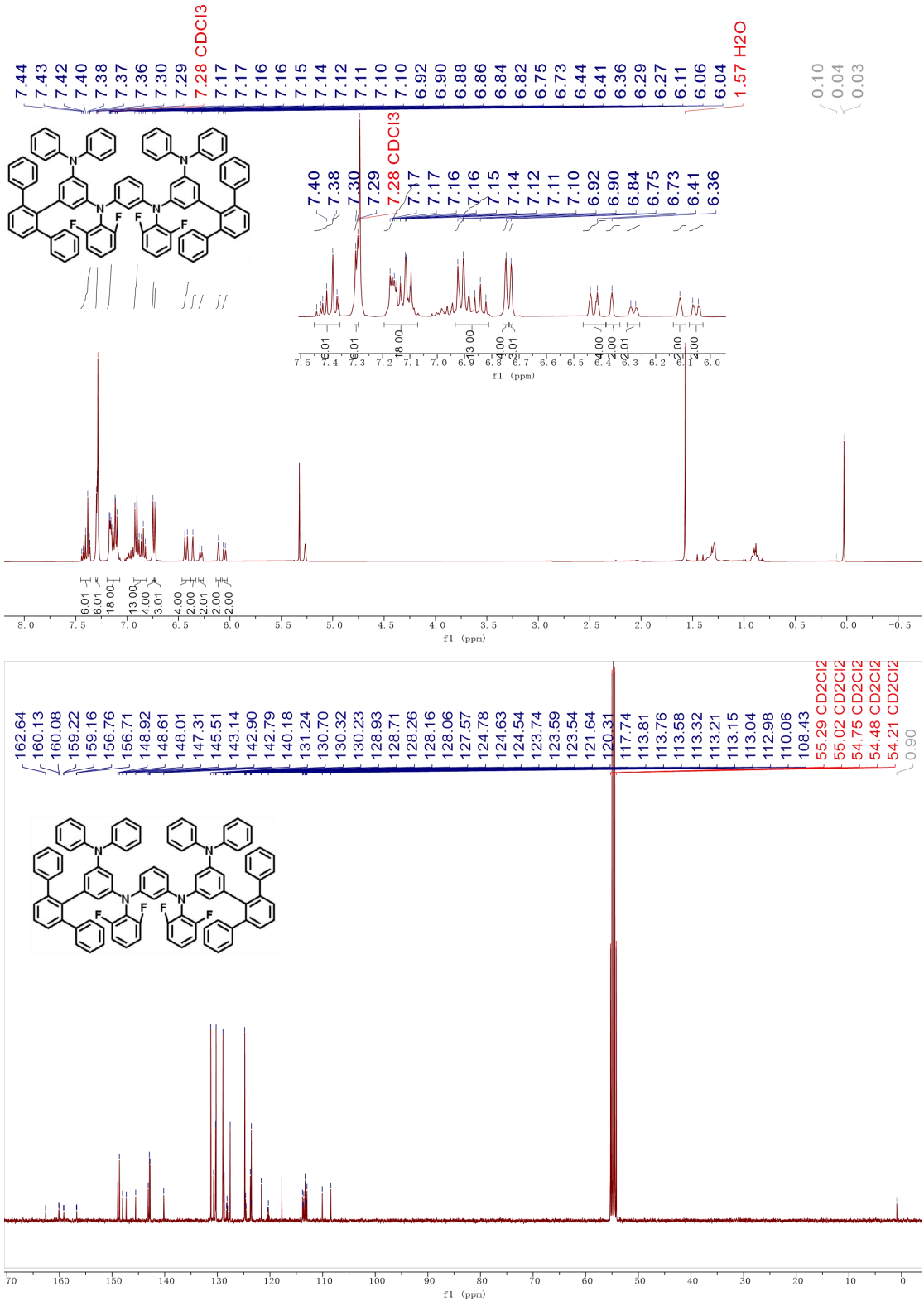

Figure S2. ^{1}H NMR and ^{13}C NMR spectrum of compound 6.

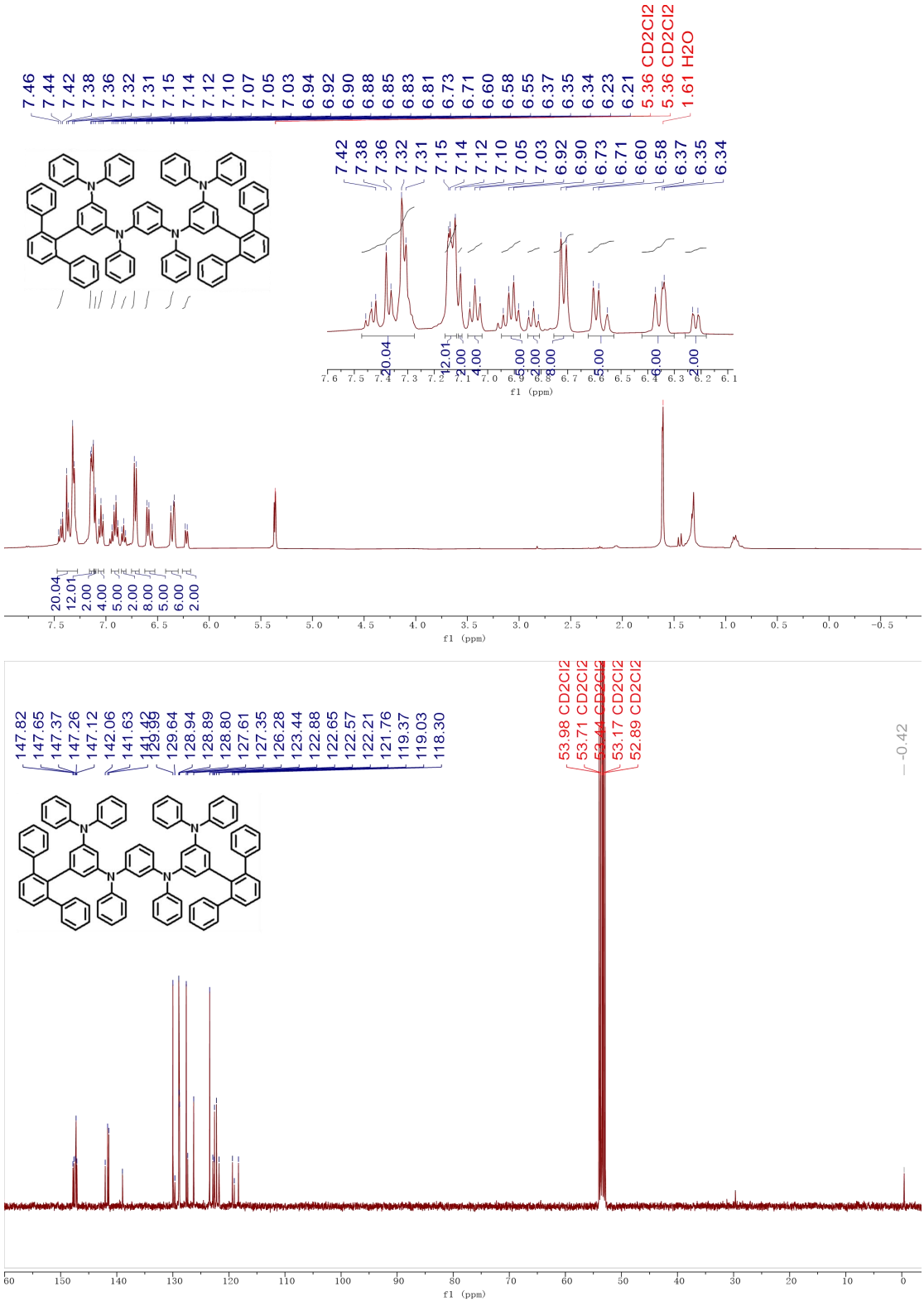

Figure S3. ^{1}H NMR and ^{13}C NMR spectrum of compound 7.

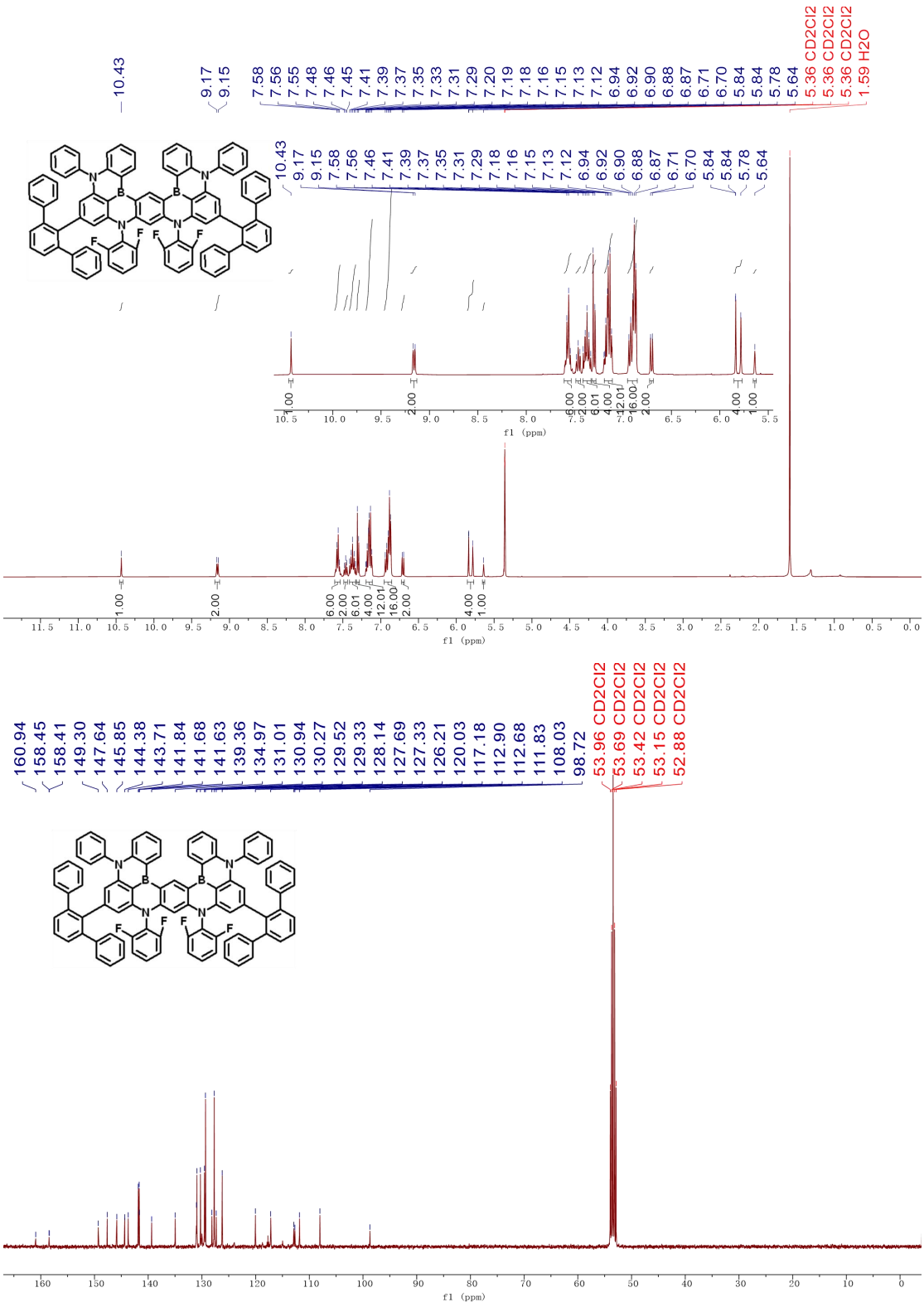

Figure S4. ^{1}H NMR and ^{13}C NMR spectrum of DTPF-ν-DABNA.

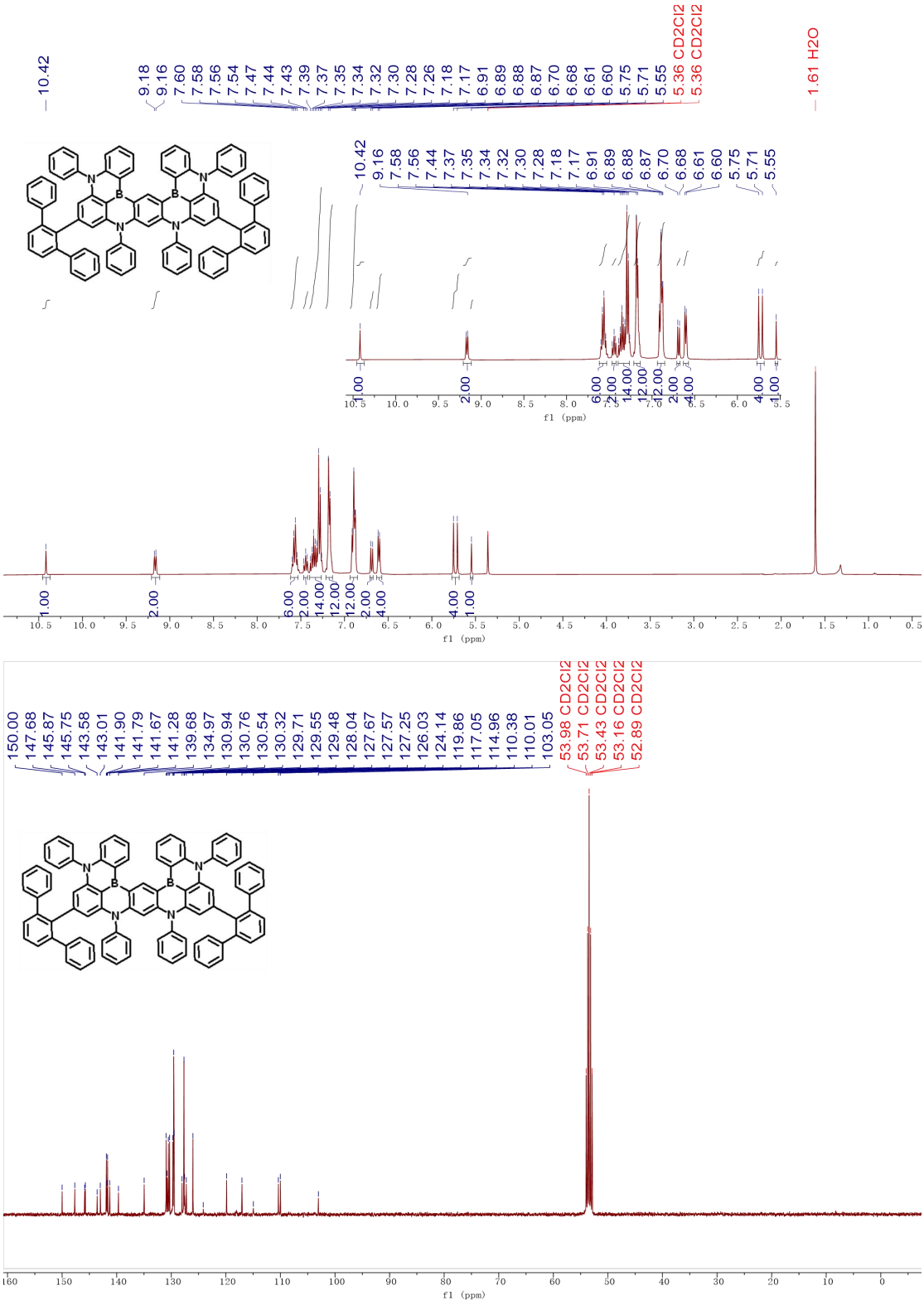

Figure S5. ^{1}H NMR and ^{13}C NMR spectrum of compound DTP-ν-DABNA.

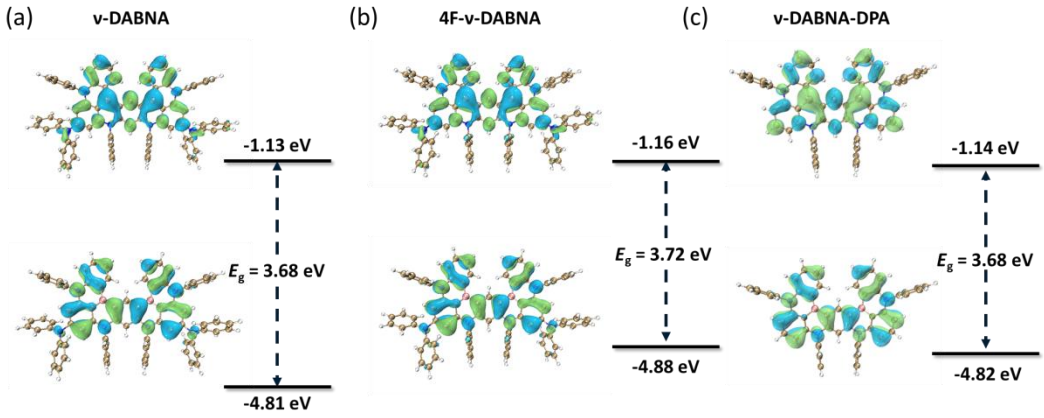

Figure S6. Calculation results of (a) ν-DABNA; (b) 4F-ν-DABNA and (c) ν-DABNA without diphenylamine

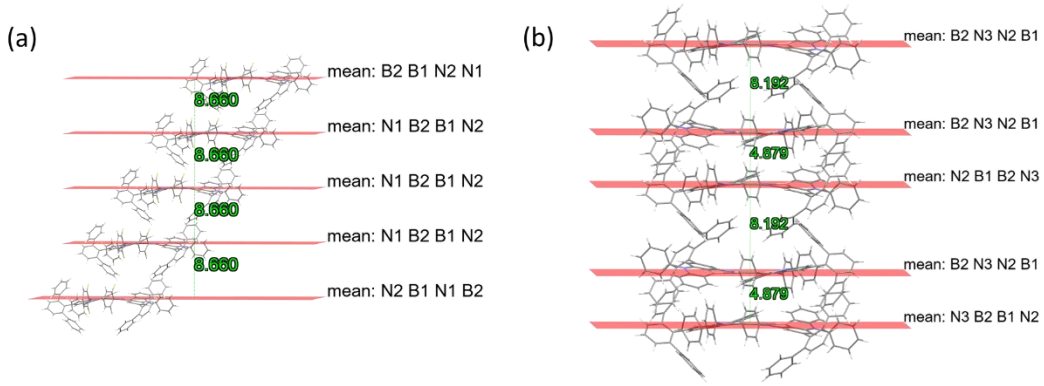

Figure S7. Packing mode of DTPF-ν-DABNA (a) and DTP-ν-DABNA (b).

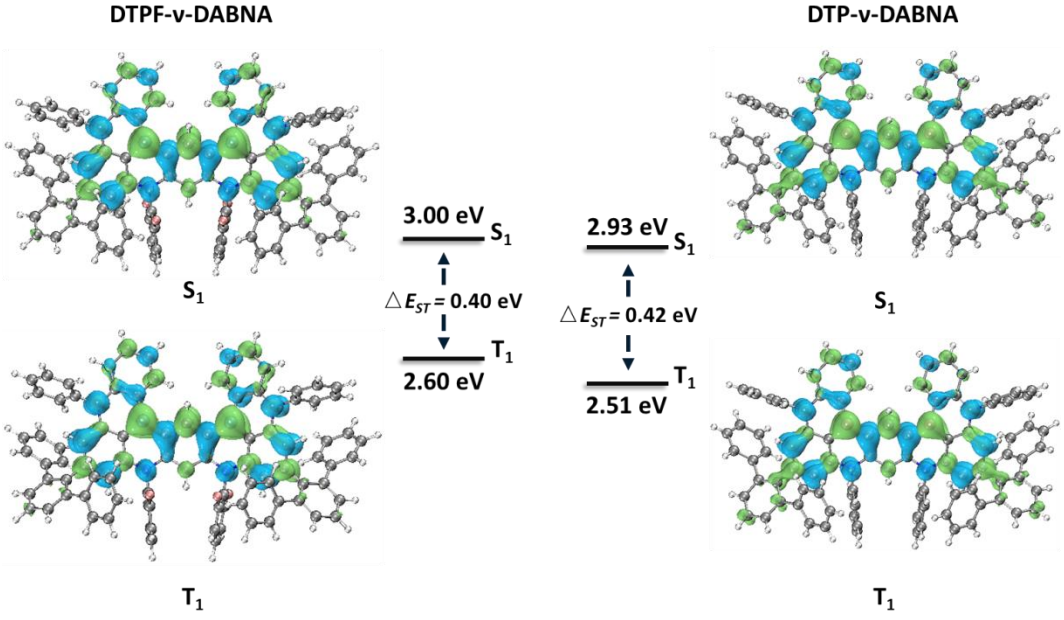

Figure S8. Excited states of DTPF-ν-DABNA and DTP-ν-DABNA.

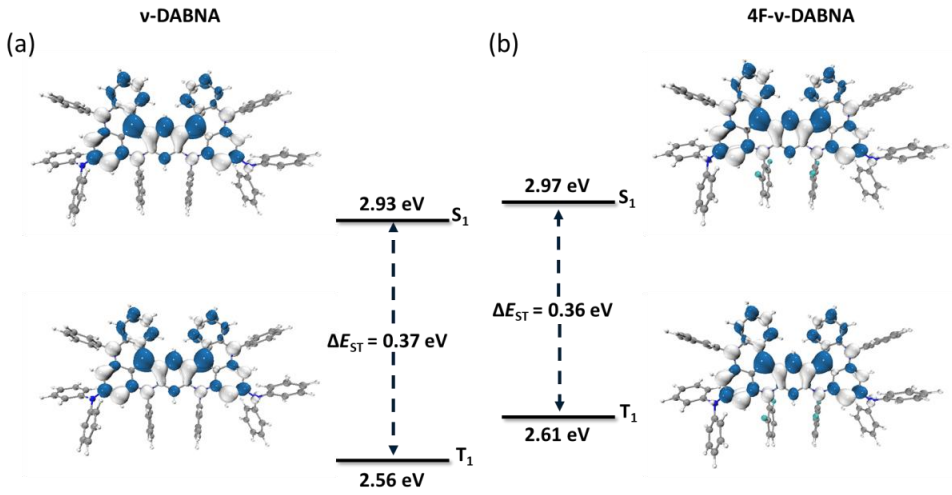

Figure S9. Excited states of ν-DABNA and 4F-ν-DABNA.

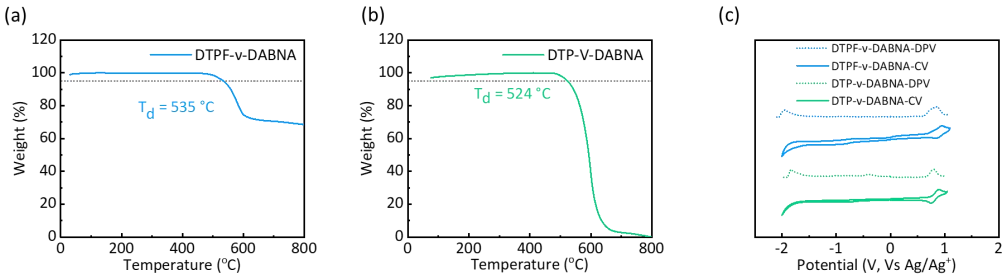

Figure S10. TGA of DTPF-ν-DABNA (a) and DTP-ν-DABNA (b); CV (c) curve of DTPF-ν-DABNA and DTP-ν-DABNA.

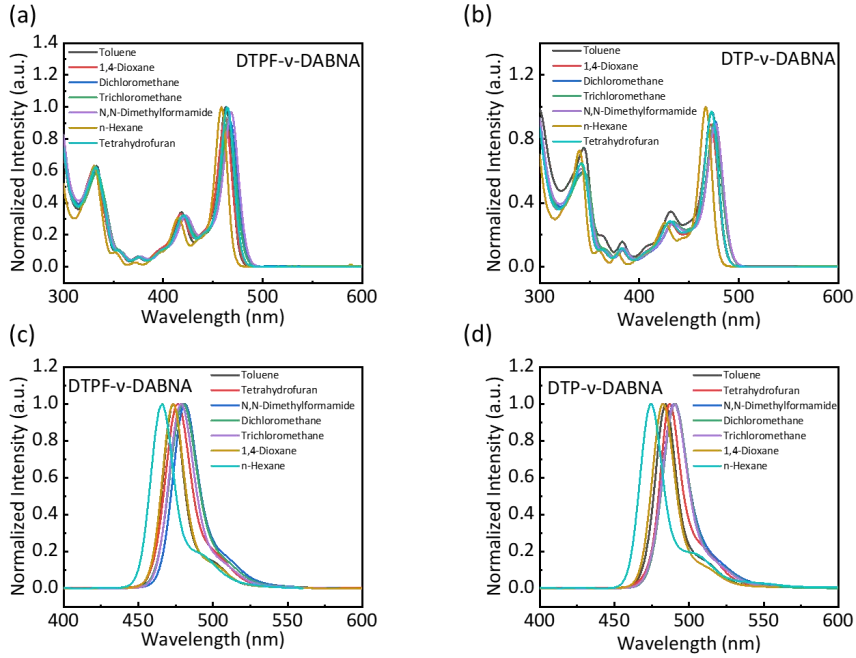

Figure S11. Absorption and fluorescence spectra of (a, c) DTPF-ν-DABNA and (b, d) DTP-ν-DABNA in various solvents (toluene, tetrahydrofuran, N,N-Dimethylformamide, dichloromethane, trichloromethane, 1,4-Dioxane and n-Hexane).

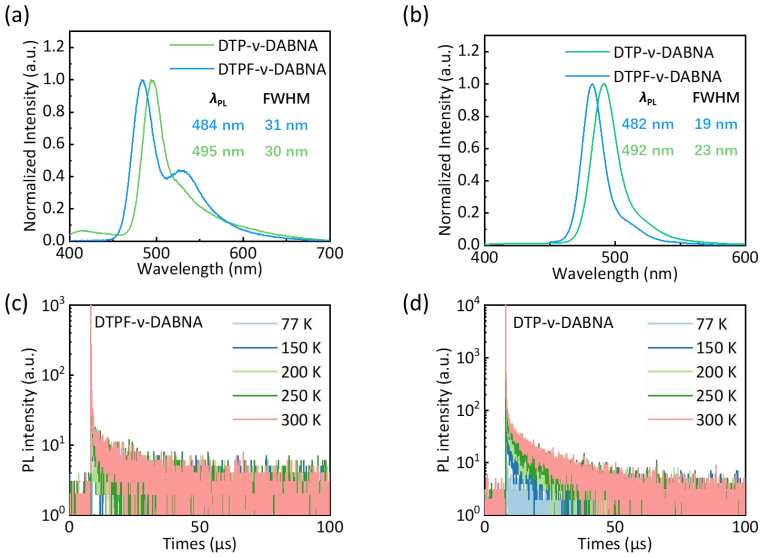

Figure S12. Fluorescence spectra of DTPF-ν-DABNA and DTP-ν-DABNA (a) PPF (2 wt% doped film) and (b) neat film, transient spectra of (c) DTPF-ν-DABNA and (d) DTP-ν-DABNA in PPF (2 wt% doped film) at different temperatures from 77 to 300 K.

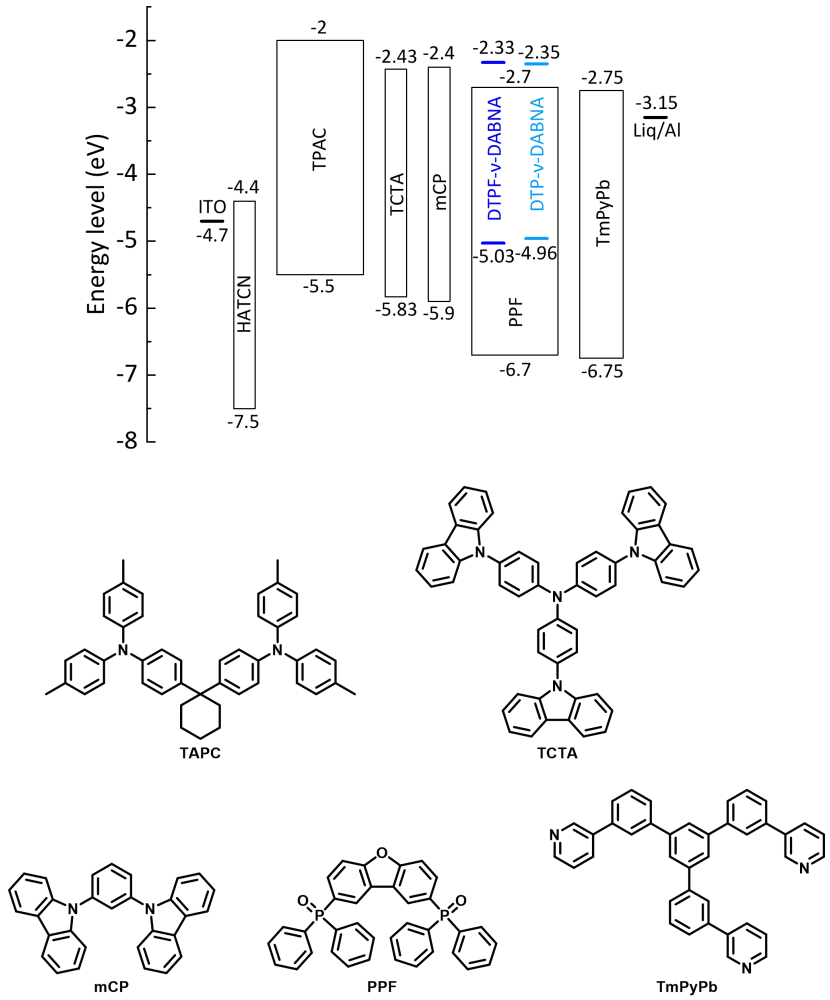

Figure S13. Energy-level diagram and chemical structures of the materials for the OLEDs based on DTPF-ν-DABNA and DTP-ν-DABNA as MR-TADF emitters.

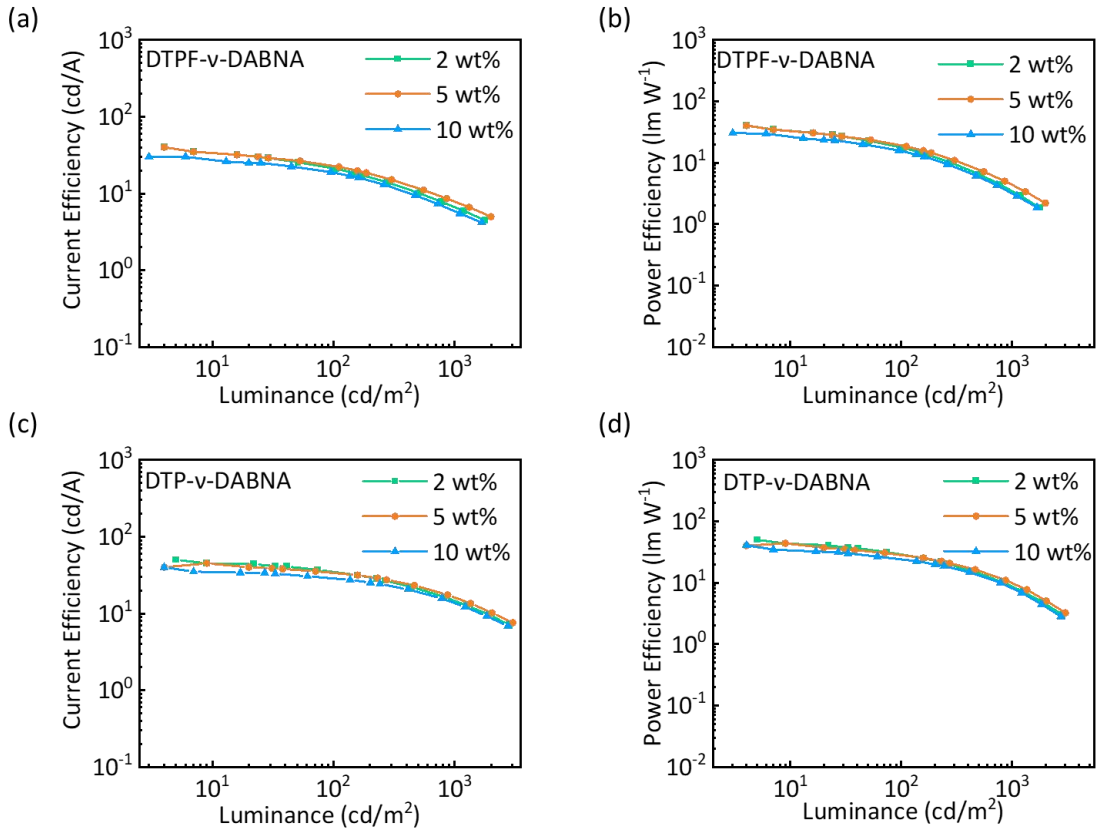

Figure S14. CE versus PE versus luminance characteristics. CE: current efficiency; PE: power efficiency.

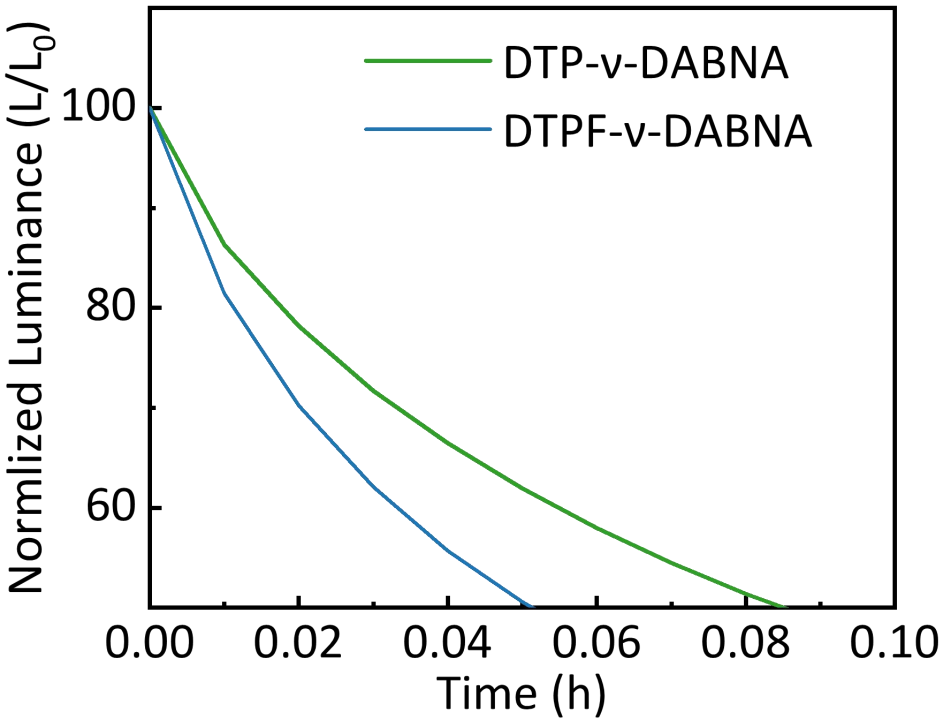

Figure S15. Device lifetime of DTPF-v-DABNA and DTP-v-DABNA.

Table S1. Crystal parameters for DTPF-ν-DABNA and DTP-ν-DABNA.

Identification code	DTPF-ν-DABNA	DTP-ν-DABNA
Empirical formula	$C_{90}H_{56}B_2F_4N_4$	$C_{90}H_{60}B_2N_4$
Formula weight	1291	1219.04
Temperature/K	170	100
Crystal system	monoclinic	triclinic
Space group	$P2_1/c$	P-1
a/Å	17.1615(8)	13.8558(11)
b/Å	14.0010(6)	16.8935(15)
c/Å	33.9349(16)	21.1023(18)
α/°	90	102.224(3)
β/°	101.338(2)	104.161(2)
γ/°	90	108.425(2)
Volume/Å^3	7994.7(6)	4313.7(6)
Z	4	2
ρ_{calc}g/cm^3	1.073	0.939
μ/mm^{-1}	0.068	0.054
F(000)	2680	1276
Crystal size/mm^3	0.15 × 0.08 × 0.05	0.12 × 0.07 × 0.04
Radiation	MoKα (λ = 0.71073)	MoKα (λ = 0.71073)
2Θ range for data collection/°	3.828 to 51.422	3.884 to 52.884
Index ranges	-20 ⩽ h ⩽ 20, -17 ⩽ k ⩽ 16, -39 ⩽ l ⩽ 41	-15 ⩽ h ⩽ 17, -21 ⩽ k ⩽ 20, -26 ⩽ l ⩽ 26
Reflections collected	51828	45482
Independent reflections	14904 [R_{int} = 0.0801, R_{sigma} = 0.0827]	17247 [R_{int} = 0.0683, R_{sigma} = 0.0938]
Data/restraints/parameters	14904/0/901	17247/0/865
Goodness-of-fit on F^2	1.039	1.048
Final R indexes [I>=2 σ (I)]	R_1 = 0.0553, wR_2 = 0.1294	R_1 = 0.0958, wR_2 = 0.2628
Final R indexes [all data]	R_1 = 0.1013, wR_2 = 0.1487	R_1 = 0.1521, wR_2 = 0.2974
Largest diff. peak/hole / e Å^{-3}	0.21/-0.22	0.66/-0.39

Table S2. Photophysical properties of DTP-ν-DABNA and DTPF-ν-DABNA.

Solvent	DTPF-ν-DABNA		DTP-ν-DABNA	
	λ_{PL} nm	FWHM nm	λ_{PL} nm	FWHM nm
n-Hexane	466	18	474	18
Toluene	474	16	484	17
1,4-Dioxane	473	17	482	18
Tetrahydrofuran	477	20	487	17
Trichloromethane	478	20	490	17
Dichloromethane	480	22	491	20
N,N-Dimethylformamide	481	20	490	21

Table S3. Photophysical properties DTP-ν-DABNA and DTPF-ν-DABNA in doped PPF films (2 wt%).

Compound	Φ_{PF}/Φ_{DF} %/%	τ_{PF}/τ_{DF} ns/μs	k_{PF} $\times 10^8$ s^{-1}	k_{DF} $\times 10^4$ s^{-1}	k_r^S $\times 10^8$ s^{-1}	k_{ISC} $\times 10^7$ s^{-1}	k_{RISC} $\times 10^5$ s^{-1}	k_{nr}^S $\times 10^6$ s^{-1}
DTPF-ν-DABNA	67.4/31.8	3.40/11.66	2.94	8.58	1.98	9.41	1.26	1.60
DTP-ν-DABNA	53.4/42.1	2.98/13.15	3.36	7.60	1.79	14.8	1.36	8.44

In this work, the doped films of DTP-ν-DABNA and DTPF-ν-DABNA do not exhibit phosphorescence emission at 300 K. In other words, the efficiency of phosphorescence is zero ($\Phi_{Phos} = 0$). Thus, the quantum efficiency of delayed emission (Φ_{DE}) is equal to the efficiency of delayed fluorescence (Φ_{DF}). Thus, the quantum efficiencies of prompt (Φ_{PF}) and delayed emission (Φ_{DF}) are evaluated by the corrected estimation method and the rate constants were calculated according to the reported method[4].

$$k_{PF} = \frac{1}{\tau_{PF}}$$

$$k_{DF} = \frac{1}{\tau_{DF}}$$

$$k_r^S = k_{PF}\Phi_{PF}$$

$$k_{nr}^S = k_{PF}\frac{\Phi_{PF}}{\Phi_{all}}(1 - \Phi_{all})$$

$$k_{ISC} = k_{PF}\frac{\Phi_{DF}}{\Phi_{all}} - k_{DF}\frac{\Phi_{DF}}{\Phi_{PF}}$$

$$k_{RISC} = k_{DF}\frac{\Phi_{all}}{\Phi_{PF}}$$

$$k_{nr}^{T} = 0$$

where k_{PF} and k_{DF} are the radiative decay rate for prompt and delayed fluorescence, respectively, Φ_{all} is the total photoluminescence quantum efficiency, K_r^S and k_{nr}^S are the radiative and nonradiative decay rate constants from a singlet excited state, respectively, k_{ISC} and k_{RISC} are the intersystem crossing and reverse intersystem crossing rate constants, respectively, k_{nr}^T is the nonradiative decay rate constant from a triplet excited state.

Table S4. Summary of OLED device performance utilizing **ν-DABNA**, DTPF-ν-DABNA and DTP-ν-DABNA.

Dopant	**x (wt%)**	**$CE_{max/10/100/1000}$ (cd A^{-1})**	**$PE_{max/10/100/1000}$ (lm W^{-1})**	**EQE $_{max/10/100/1000}$ (%)**
ν-DABNA	1	31.0/-/29.5/23.2	25.6/-/20.8/11.7	34.4/-/32.8/26.0
DTPF-ν-DABNA	2	40.0/33.7/22.8/7.8	40.5/33.1/19.3/4.4	36.0/28.9/18.5/6.3
	5	40.0/33.7/21.3/6.6	40.4/32.8/17.8/3.4	34.2/27.3/18.2/5.7
	10	30.0/27.3/18.6/5.9	30.4/26.5/15.6/3.0	24.6/21.2/14.6/4.6
DTP-ν-DABNA	2	50.0/44.7/34.8/16.2	50.0/43.2/28.8/9.9	31.5/27.0/20.9/9.1
	5	44.9/44.2/33.7/14.5	43.7/42.9/28.2/8.5	25.6/25.1/19.1/8.7
	10	40.0/34.6/28.6/13.5	40.8/33.8/24.1/8.0	22.7/18.8/15.4/7.4

Values of CE, PE, and EQE at the maximum, 10/100/1000 cd m^{-2}. CE: current efficiency; PE: power efficiency; EQE: external quantum efficiency.

Table S5 Summary of reported diboron blue MR-TADF emitters with high efficiency (EQE_{max} > 30%).

Emitters	λ_{EL} (nm)	FWHM (nm)	EQE_{max} (%)	CIE (x, y)	Ref.
DTPF-ν-DABNA	480	21	36.0	(0.09, 0.22)	This work
DTP-ν-DABNA	492	22	31.5	(0.07, 0.38)	
CFDBCz	488	22	32.4	(0.12, 0.43)	Adv. Opt. Mater. 2024, 12(15):2302987.
ν-DABNA	469	18	34.4	(0.12, 0.11)	Nat. Photon. 2019, 13(10):678-682.
NO-DBMR	469	26	33.7%	(0.12, 0.12)	Angewandte Chemie International Edition. 2023, 62(32):e202306768.
Π-CzBN	494	21	37.4	(0.08, 0.45)	Angewandte Chemie International Edition. 2023, 62(32):e202306413.
DTBA-B2N3	475	28	30.9	(0.11,0.18)	Nat. Photon. 2023, 17(3):280-285.
o-Tol-ν-DABNA-Me	472	18	33.1	(0.11, 0.12)	Sci. Adv. 2023, 9(22):eadf1388.
m-ν-DABNA	471	18	36.2	(0.12, 0.12)	
4F-ν-DABNA	464	18	35.8	(0.13, 0.08)	Chem. Eng. J. 2022, 432:134381.
4F-mν-DABNA	461	18	33.7	(0.13, 0.06)	
m[B-N]N1	478	30	30.4	(0.13, 0.27)	Angewandte Chemie International Edition. 2022, 61(40):e202207293.

References

1.Wang C, Kang X, Dai S, Cui F, Li Y, Mu H, et al. Efficient suppression of chain transfer and branching via C(s) -type shielding in a neutral nickel(II) catalyst. Angew. Chem Int Ed. 2021;60(8):4018-4022. [DOI:10.1002/anie.202013069]

2.Schlütter F, Nishiuchi T, Enkelmann V, Müllen K. π-Congested poly(paraphenylene) from 2,2′,6,6′-tetraphenyl-1,1′-biphenyl units: synthesis and structural characterization. Polym Chem. 2013;4(10):2963-2967. [DOI:10.1039/c3py00166k]

3.Naveen KR, Lee H, Braveenth R, Yang KJ, Hwang SJ, Kwoin JH. Deep blue diboron embedded multi-resonance thermally activated delayed fluorescence emitters for narrowband organic light emitting diodes. Chem Eng J. 2022;432:134381. [DOI:10.1016/j.cej.2021.134381]

4.Tsuchiya Y, Diesing S, Bencheikh F, Wada Y, Santos PL, Kaji H, et al. Exact solution of kinetic analysis for thermally activated delayed fluorescence materials. J Phys Chem Lett. 2021;125(36):8074-8089. [DOI:10.1021/acs.jpca.1c04056]